Canadian Journal of Pure and Applied Sciences
Vol. 13, No. 3, pp. 4907-4921, October 2019
Online ISSN: 1920-3853; Print ISSN: 1715-9997
Available online at www.cjpas.net

# MHD CONVECTIVE FLOW OF JEFFREY FLUID IN A PARALLEL PERMEABLE MOVING PLATE

*KW Bunonyo[1] and RI Ndu[2]
[1]Department of Mathematics and Statistics, Federal University Otuoke, Yenagoa, Bayelsa State, Nigeria
[2]Department of Mathematics, Rivers State University, Port Harcourt, Nigeria

## ABSTRACT

This research investigated the MHD Convective Flow of Jeffrey Fluid in a Parallel Permeable Moving Plate. The formulated partial differential equations were solved using perturbation technique and velocity and temperature profiles are obtained. Numerical simulation was done out using Mathematica 10.3 and the study of the flow with some physical parameters such as $Gr, Pr, M, Da$ and other pertinent parameters $Q, A, \omega, \lambda, \varepsilon$ influence on the velocity and temperature profiles. It was observed that the variation of the pertinent parameters influences the flow profiles, as it leads to increasing velocity profile with parameters $Da, Gr, up, \varepsilon$ .

**Keywords:** MHD, oscillatory, Jeffrey, convective, grashof number, hartmann number, suction parameter.

## INTRODUCTION

Most fluids used in industries show non-Newtonian qualities; consequently, analysts nowadays days are more and more intrigued by such fluid as non-Newtonian and their components. A fluid, for instance, non-Newtonian shows various properties that are distinctive a few alternative ways from the Newtonian fluids. Oftentimes we have seen that the consistency of non-Newtonian fluids is dependent on the shear rate. Some non-Newtonian fluids with shear-autonomous consistency, but still show non-Newtonian behavious. Several salt solution and fluid polymers are non-Newtonian fluids as are frequently discovered substances, for instance, ketchup, custards and toothpaste, starch suspensions, foodstuff, slurries, beauty care merchandise and toiletries, maizena, paint, blood and cleansing agent so on. The non-Newtonians fluid is likewise very useful in several designing applications. The various kinds of non-Newtonian fluids are Casson liquid, Jeffrey fluid, visco-elastic fluid, couple pressure fluid, small scale polar fluid, control law fluid. Among these fluids, the foremost widely known is the Jeffrey fluid Hayat *et al*. (2012). In recent times, the model received distinctive attractions from the researchers such as Hayat *et al*. (2008). Ahmed *et al*. (2015) investigated the convective heat transfer of magneto-hydodynamics (MHD) Jeffrey fluid over a stretching sheet. Thereafter, hydrokinetics mixed convection flow and heat transfer of a Jeffrey fluid over an exponentially stretched plate was investigated by Ahmed *et al*. (2016). The unsteady MHD free flow of a Casson fluid with constant wall temperature was analyzed by Khalid *et al*. (2015).

Moreover, mixed convective flow of power law fluids on a vertical wavy surface in the presence of a transversal magnetic flux was conjointly investigated by Nejad *et al*. (2015). Berman (1953) studied the streamline flow in channel with porous walls. Kirubhashankar and Ismail (2014) thought of the magnetic flux within the streamline flow of an electrically conducting liquid. Hassanien and Manour (1990) have investigated the magnetic flow through the porous medium between two infinite plates. Hamza (1999) has studied the suction and injection effects of flow between parallel plates. Soundalgekar and Uplekar (1986) studied the result of heat transfer considering constant temperature. Singh and Ram (1978) thought of streamline flow of an electrically conducting fluid through a channel within the presence of transversal magnetic flux underneath the influence of periodic pressure

*Corresponding author e-mail: wilcoxbk@fuotuoke.edu.ng

gradient and resolved the governing equation by the tactic of Pierre Simon de Laplace rework. The requirements of recent machinery have motivated the interest in fluid flow studies, which involve the interaction of many phenomena.

One such study is given, once a viscous fluid flows over a porous surface has its significance in several engineering issues like flow of liquid in a very porous bearing Joseph and Tao (1966), within the field of water in fluid channel beds, in oil technology to check the movement of gas, oil and water through the oil reservoirs, in chemical engineering for filtration and purifications method. Cunningham and Williams (1980) conjointly reportable many geology applications of flow in porous medium, viz. porous rollers and its natural prevalence within the flow of rivers through porous banks and beds and also the flow of oil through underground porous rocks. Brinkman (1949) planned modification of the Darcy's law for porous medium. In most of the examples, the fluid flows through porous medium, have two regions.

In region I, the fluid is unengaged to flow and in region II, the fluid flows through the porous medium Cox (1991). Bunonyo *et al*. (2017) investigated flow of blood although a channel by presumptuous the Jeffrey fluid to be blood and analyze the obtained results. Moreover, Emeka *et al*. (2019) conjointly researched on heat and mass transfer of MHD free convective dissipation with heat absorption and reaction result. Bunonyo *et al*. (2019) investigated the periodic MHD elastic flow in a very porous channel with heat in the presence of magnetic flux. The developed equations were resolved analytically using perturbation technique to get the velocity and temperature profiles. During this analysis, we have a tendency to investigated MHD convective flow of Jeffrey fluid in a very parallel porous moving plate as we developed governing equations by considering oscillation on the perturbed momentum and energy equations, thenceforth we have a tendency to acquire the velocity and temperature profiles analytically with some pertinent parameters concerned. Furthermore, investigate if those parameter influences the flow behaviors as it progresses at the boundary surface and away from it.

## MATHEMATICAL FORMULATION

We consider an MHD Convective Flow of Jeffrey Fluid in Parallel Permeable Moving Plates. It is assumed that the fluid is electrically conducting, incompressible and heat absorbing. The flow is directed towards the $x'$ axis and $y'$ axis perpendicular to the direction of fluid flow. A uniform magnetic field is applied normal to the flow direction. It is assumed that the upper plate is moving with a velocity $up$, oscillating temperature and is varying with time. Under the said assumptions the boundary layer equation of velocity and temperature are given as:

$$v' = -V_o\left(1+\varepsilon A e^{n't'}\right) \quad (1)$$

$$\frac{\partial u'}{\partial t'} + v'\frac{\partial u'}{\partial y'} = \frac{\upsilon}{1+\lambda}\frac{\partial^2 u'}{\partial y'^2} - \left(\frac{\sigma B_0^2}{\rho} + \frac{\upsilon}{k'}\right)u' + g\beta_T\left(T' - T'_\infty\right) \quad (2)$$

$$\frac{\partial T'}{\partial t'} + v'\frac{\partial T'}{\partial y'} = \frac{k_T}{\rho c_p}\frac{\partial^2 T'}{\partial y'^2} - \frac{Q_0}{\rho Cp}\left(T' - T'_\infty\right) \quad (3)$$

The corresponding boundary conditions are as:

$$\left.\begin{array}{lll} u' = u'_p, & T' = T'_\infty + \left(T'_w - T'_\infty\right)\mathrm{e}^{\omega' t'} & \text{on } y' = 0 \\ u' \to 0, & T' \to T'_\infty & \text{on } y' \to \infty \end{array}\right\} \quad (4)$$

The following non-dimensional parameters are introduced as:

$$\left.\begin{array}{l} u = \dfrac{u'}{V_0}, y = \dfrac{V_o y'}{\upsilon}, n = \dfrac{n'\upsilon}{V_o^2}, \omega = \dfrac{\omega'\upsilon}{V_o^2}, t = \dfrac{t'V_0^2}{\upsilon}, \\ Pr = \dfrac{\mu Cp}{k_T}, v = \dfrac{v'}{V_o} k = \dfrac{k'V_o^2}{\upsilon^2}, \theta = \dfrac{T' - T'_\infty}{T'_w - T'_\infty}, M^2 = \dfrac{a^2\sigma_e B_o^2}{\rho V_o^2}, \\ Q = \dfrac{Q_0\upsilon}{\rho Cp V_o^2}, Gr = \dfrac{g\beta_T\left(T'_w - T'_\infty\right)}{V_o^3}, up = \dfrac{up'}{V_o} \end{array}\right\} \quad (5)$$

We transformed equations (2) and (3) using the corresponding dimensional parameters in equation (5) as:

$$\frac{\partial u}{\partial t} + \left(1+\varepsilon A e^{nt}\right)\frac{\partial u}{\partial y} = \frac{1}{1+\lambda}\frac{\partial^2 u}{\partial y^2} - \left(M^2 + \frac{1}{Da}\right)u + Gr\theta \quad (6)$$

$$Pr\frac{\partial \theta}{\partial t} + Pr\left(1+\varepsilon A e^{nt}\right)\frac{\partial \theta}{\partial y} = \frac{\partial^2 \theta}{\partial y^2} - PrQ\theta \quad (7)$$

The corresponding boundary conditions are:

$$\left.\begin{aligned} &u = u_p, \quad \theta = e^{i\omega t} \quad \text{on } y = 0 \\ &u \to 0, \quad \theta \to 0 \quad \text{on } y \to \infty \end{aligned}\right\} \tag{8}$$

**METHOD OF SOLUTION**

In order to solve equation (6) and equation (7) in a purely oscillatory fashion, we adopt the following:

$$u = u_0 e^{i\omega t}, \theta = \theta_0 e^{i\omega t} \tag{9}$$

Putting equation (9) into equation (6) and (7) as follows:

$$\frac{\partial^2 u_0}{\partial y^2} - \left(1+\varepsilon A e^{nt}\right)(1+\lambda)\frac{\partial u_0}{\partial y} - \left(M^2 + \frac{1}{Da} + i\omega\right)(1+\lambda) u_0 = -Gr(1+\lambda)\theta_0 \tag{10}$$

$$\frac{\partial^2 \theta_0}{\partial y^2} - Pr\left(1+\varepsilon A e^{nt}\right)\frac{\partial \theta_0}{\partial y} - (Q + i\omega) Pr\theta_0 = 0 \tag{11}$$

Equations (10) and (11) can be rewritten as follows:

$$\frac{\partial^2 u_0}{\partial y^2} - \beta_1 \frac{\partial u_0}{\partial y} - \beta_2 u_0 = -\beta_3 \theta_0 \tag{10}$$

$$\frac{\partial^2 \theta_0}{\partial y^2} - \beta_4 \frac{\partial \theta_0}{\partial y} - \beta_5 \theta_0 = 0 \tag{11}$$

where $\beta_1 = \left(1+\varepsilon A e^{nt}\right)(1+\lambda)$,

$\beta_2 = \left(M^2 + \frac{1}{Da} + i\omega\right)(1+\lambda), \beta_3 = Gr(1+\lambda)$,

$\beta_4 = Pr\left(1+\varepsilon A e^{nt}\right)$,

$\beta_5 = (Q + i\omega) Pr$

$$\left.\begin{aligned} &u_0 = u_p e^{-i\omega t}, \quad \theta_0 = 1 \quad \text{at } y = 0 \\ &u \to 0, \qquad \theta \to 0 \quad \text{at } y \to \infty \end{aligned}\right\} \tag{12}$$

Solving equation (10) and (11), we have the following:

$$\theta_0 = \beta_6 e^{m_1 y} + \beta_7 e^{-m_2 y} \tag{13}$$

Where:

$$m_1 = \frac{\beta_4 + \sqrt{(\beta_4)^2 + 4\beta_5}}{2}, m_2 = \frac{\beta_4 - \sqrt{(\beta_4)^2 + 4\beta_5}}{2}$$

Putting equation (13) into equation (10) we have:

$$\frac{\partial^2 u_0}{\partial y^2} - \beta_1 \frac{\partial u_0}{\partial y} - \beta_2 u_0 = -\beta_3\left(\beta_6 e^{m_1 y} + \beta_7 e^{-m_2 y}\right) \tag{14}$$

We can now solve equation (14), the non homogenous ordinary differential equation with solution as:

$$u_0 = \beta_8 e^{J_1 y} + \beta_9 e^{-J_2 y} + \beta_{10} e^{m_1 y} + \beta_{11} e^{-m_2 y} \tag{15}$$

where

$$J_1 = \frac{\beta_1 - \sqrt{(\beta_1)^2 + 4\beta_1}}{2}, J_2 = \frac{\beta_1 + \sqrt{(\beta_1)^2 + 4\beta_1}}{2},$$

$$\beta_{10} = \frac{-\beta_3\beta_6}{m_1^2 + \beta_1 m_1 - \beta_2}, \beta_{11} = \frac{-\beta_3\beta_7}{m_2^2 + \beta_1 m_2 - \beta_2}$$

Solving for the undetermined coefficients in equations (13) and equation (14) using the corresponding boundary conditions in equation (12), we obtain the velocity and temperature profiles as:

$$\theta = \left(e^{-m_2 y}\right) e^{i\omega t} \tag{16}$$

$$u = \left(\left(u_p e^{-i\omega t} - \beta_{11}\right) e^{-J_2 y} + \beta_{11} e^{-m_2 y}\right) e^{i\omega t} \tag{17}$$

**RESULTS**

The formulated governing equations (10) and (11) with the corresponding boundary conditions are solved analytically using perturbation method involving oscillation term. In order to have physical insight of the pertinent parameters on the velocity and temperature profiles in equations (16) and (17), numerical simulation were carried out and here are results presented in Figures 1-16 in addition, we considered the following values $M = 2, Da = 0.5$, $Pr = 0.71, Gr = 10, Q = 0.2, \omega = 3, up = 0.3, t = 1$, $\lambda = 0.3$.

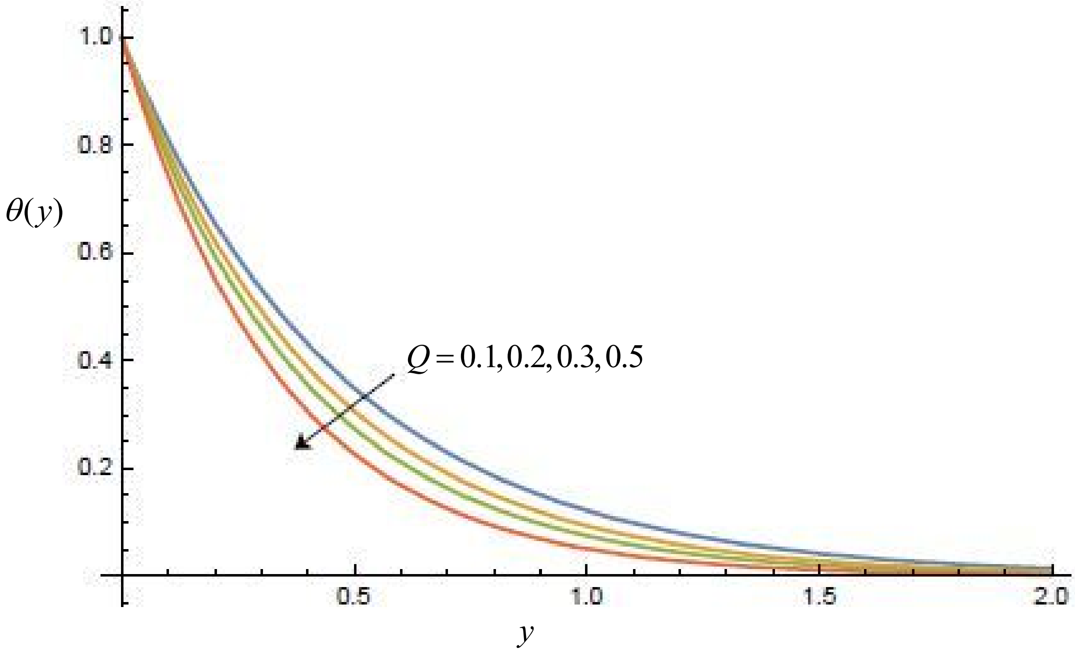


Fig. 1. Influence of $Q$ on velocity profile while other parameters values are $M = 2, Da = 0.5, Pr = 0.71, Gr = 10, A = 0.5, \omega = 3, up = 0.3, t = 1, \lambda = 0.3$

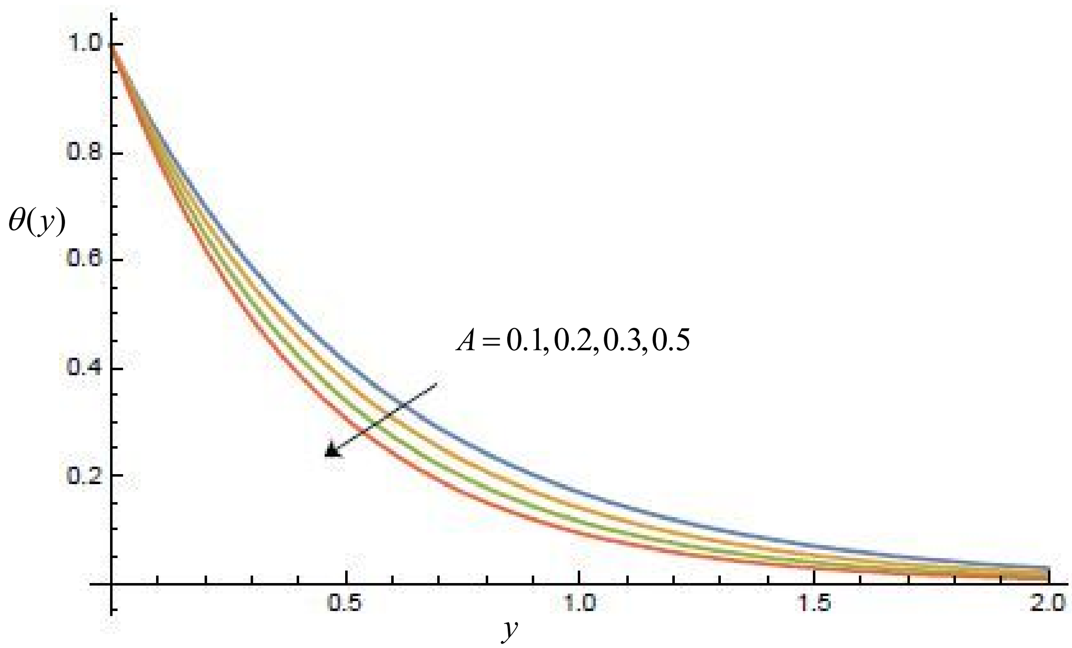


Fig. 2. Influence of $A$ on velocity profile while other parameters values are $M = 2, Da = 0.5, Pr = 0.71, Gr = 10, Q = 0.2, \omega = 3, up = 0.3, t = 1, \lambda = 0.3$

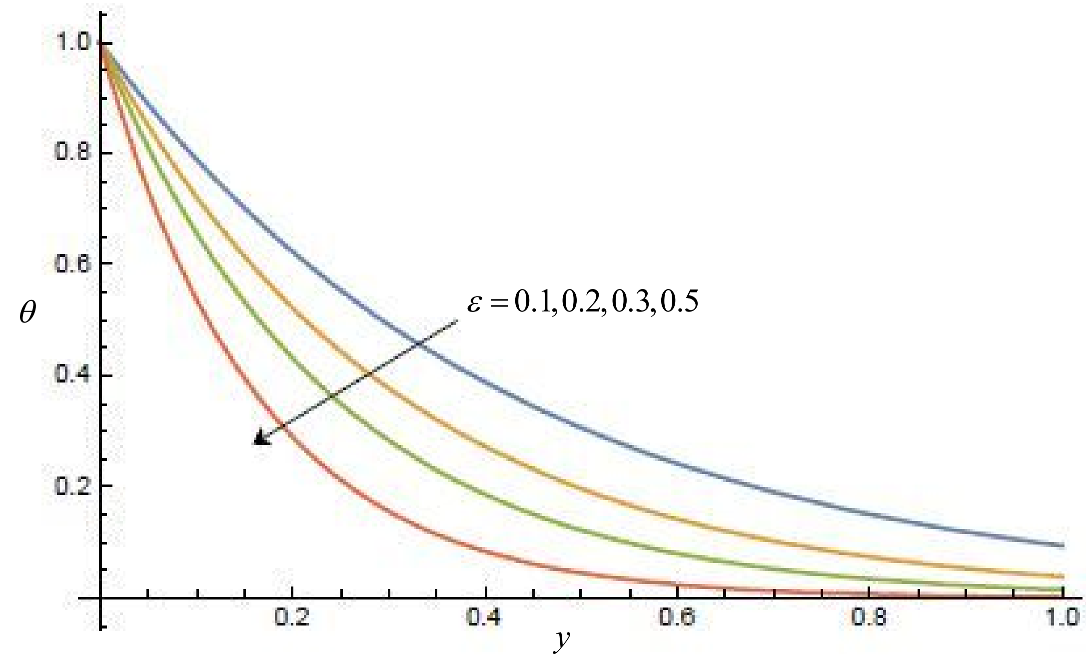


Fig. 3. Influence of $\varepsilon$ on velocity profile while other parameters values are $M = 2, Da = 0.5, Pr = 0.71, Gr = 10, Q = 0.2, \omega = 3, up = 0.3, t = 1, \lambda = 0.3$

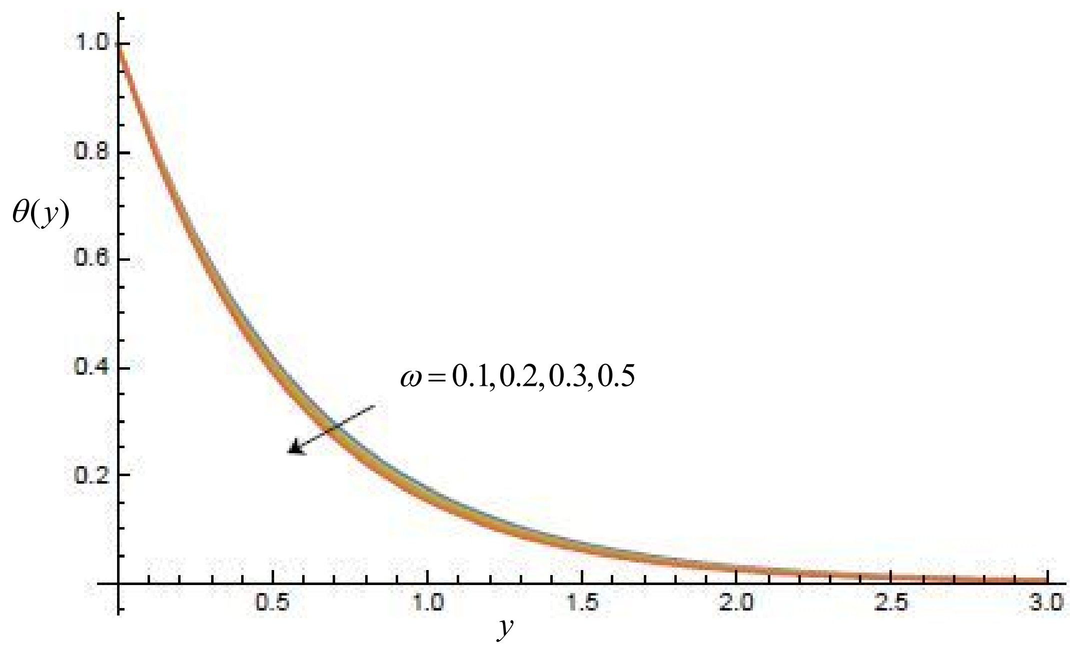


Fig. 4. Influence of $\omega$ on velocity profile while other parameters values are $M = 2, Da = 0.5, Pr = 0.71, Gr = 10, Q = 0.2, up = 0.3, t = 1, \lambda = 0.3$

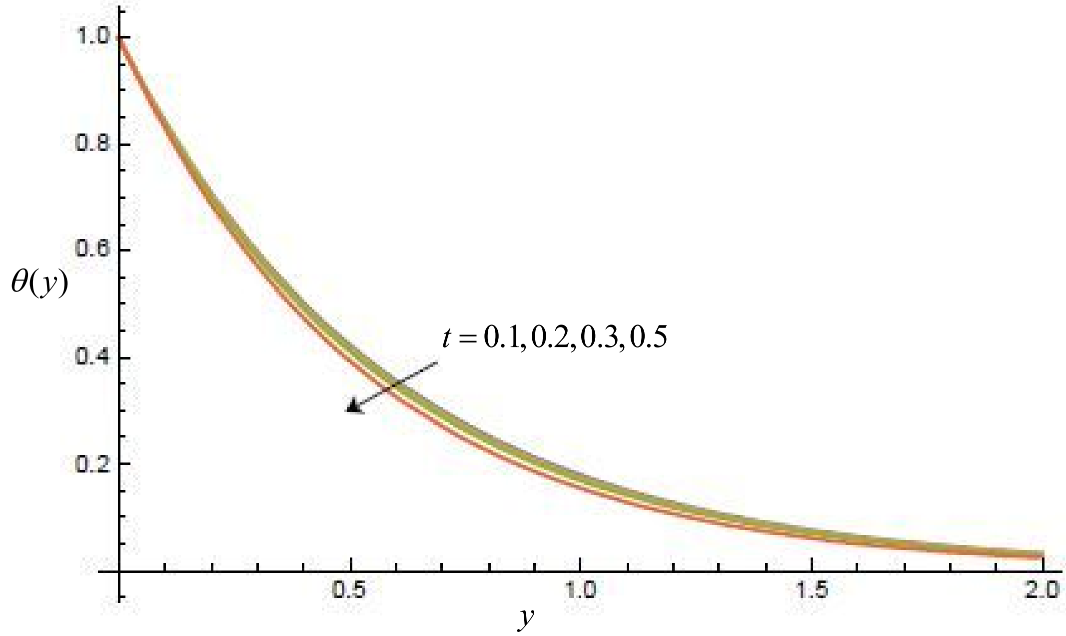


Fig. 5. Influence of $t$ on velocity profile while other parameters values are $M = 2, Da = 0.5, Pr = 0.71, Gr = 10, Q = 0.2, \omega = 3, up = 0.3, t = 1, \lambda = 0.3$

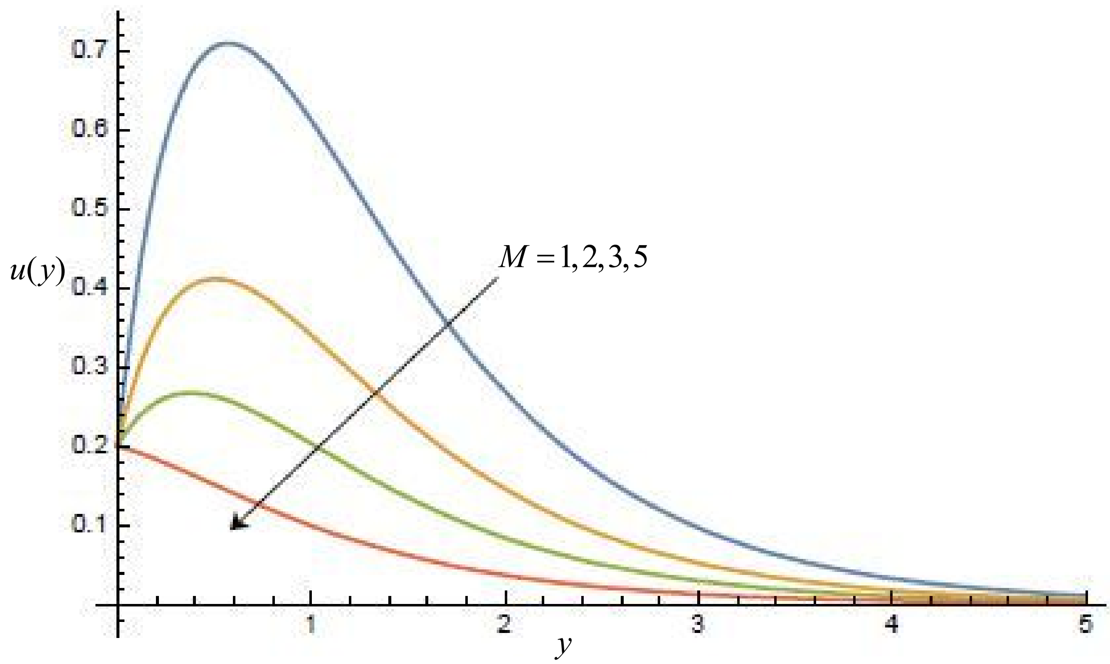


Fig. 6. Influence of $M$ on velocity profile while other parameters values are $M = 2, Da = 0.5, Pr = 0.71, Gr = 10, Q = 0.2, \omega = 3, up = 0.3, t = 1, \lambda = 0.3$

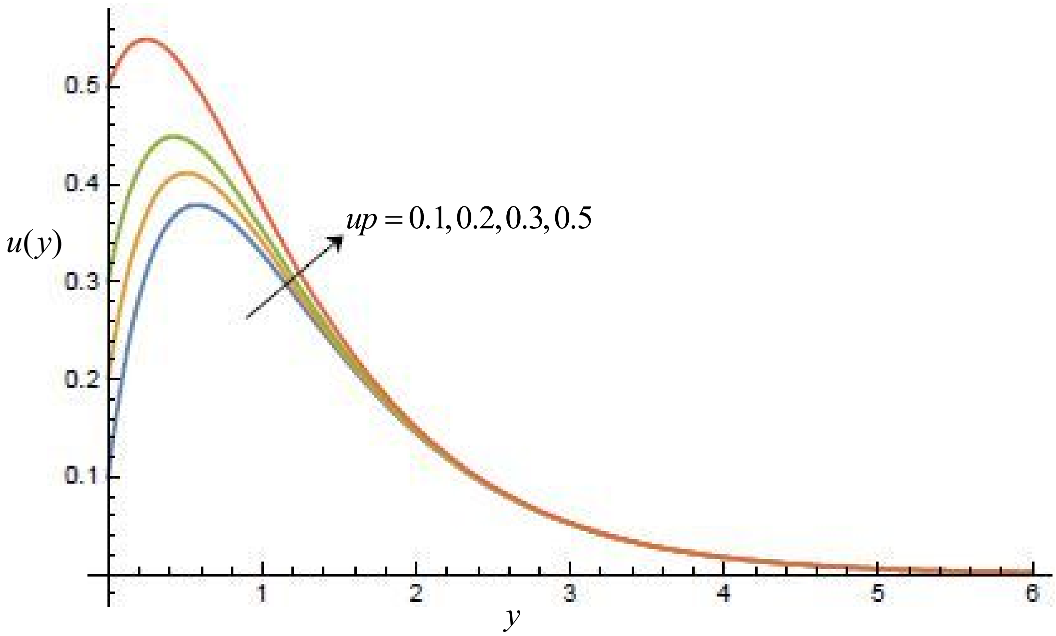


Fig. 7. Influence of $up$ on velocity profile while other parameters values are $M = 2, Da = 0.5, Pr = 0.71, Gr = 10, Q = 0.2, \omega = 3, up = 0.3, t = 1, \lambda = 0.3$

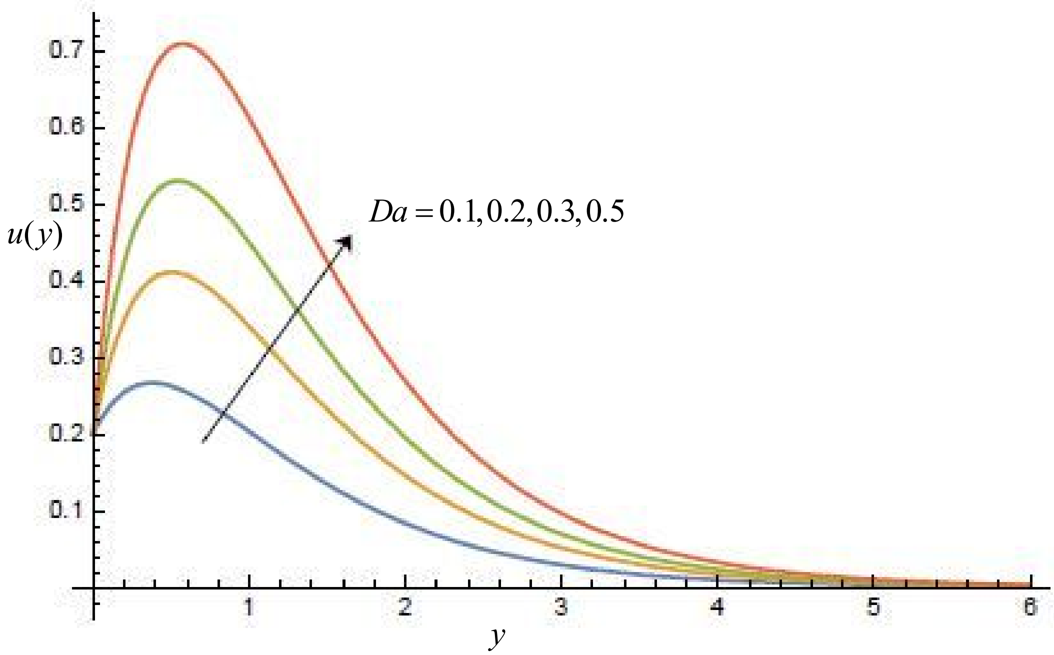


Fig. 8. Influence of $Da$ on velocity profile while other parameters values are $M = 2, Da = 0.5, Pr = 0.71, Gr = 10, Q = 0.2, \omega = 3, up = 0.3, t = 1, \lambda = 0.3$

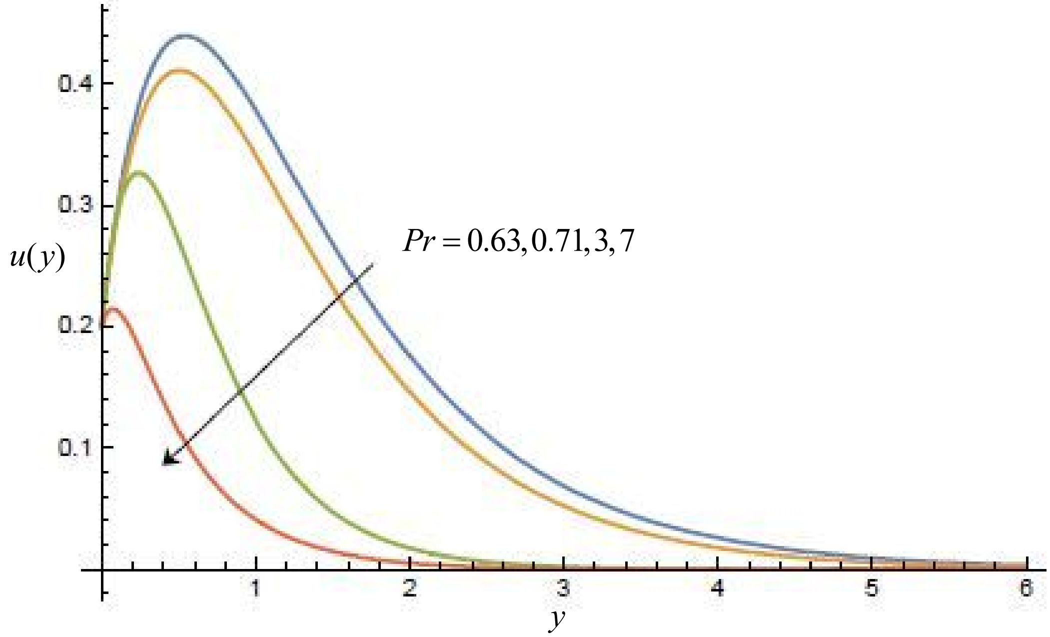


Fig. 9. Influence of $Pr$ on velocity profile while other parameters values are $M = 2, Da = 0.5, Pr = 0.71, Gr = 10, Q = 0.2, \omega = 3, up = 0.3, t = 1, \lambda = 0.3$

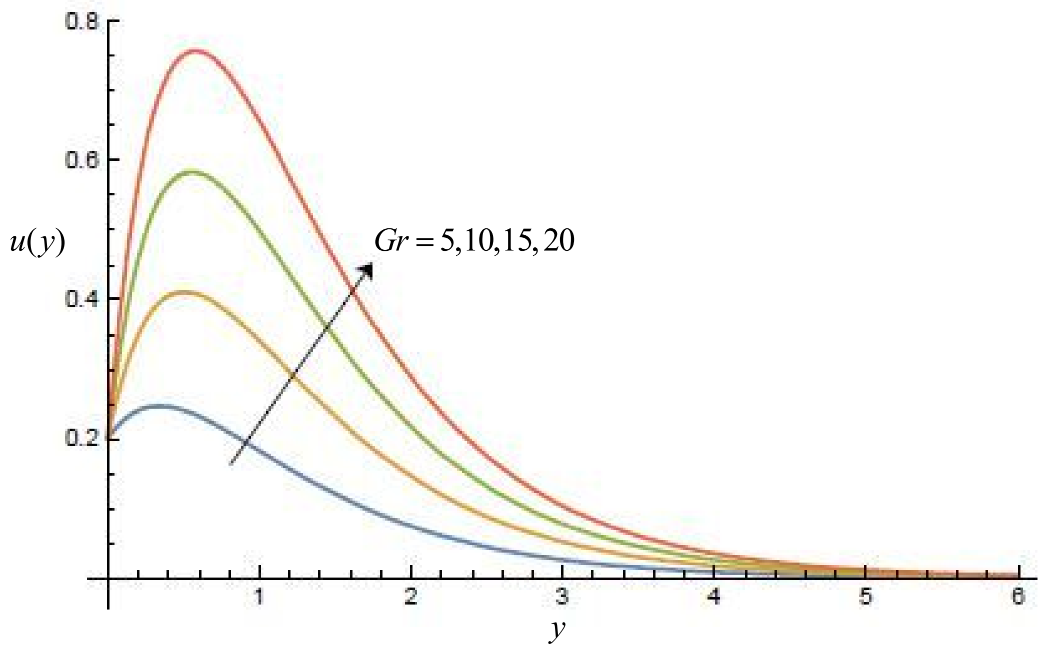


Fig. 10. Influence of $Gr$ on velocity profile while other parameters values are $M = 2, Da = 0.5, Pr = 0.71, Gr = 10, Q = 0.2, \omega = 3, up = 0.3, t = 1, \lambda = 0.3$

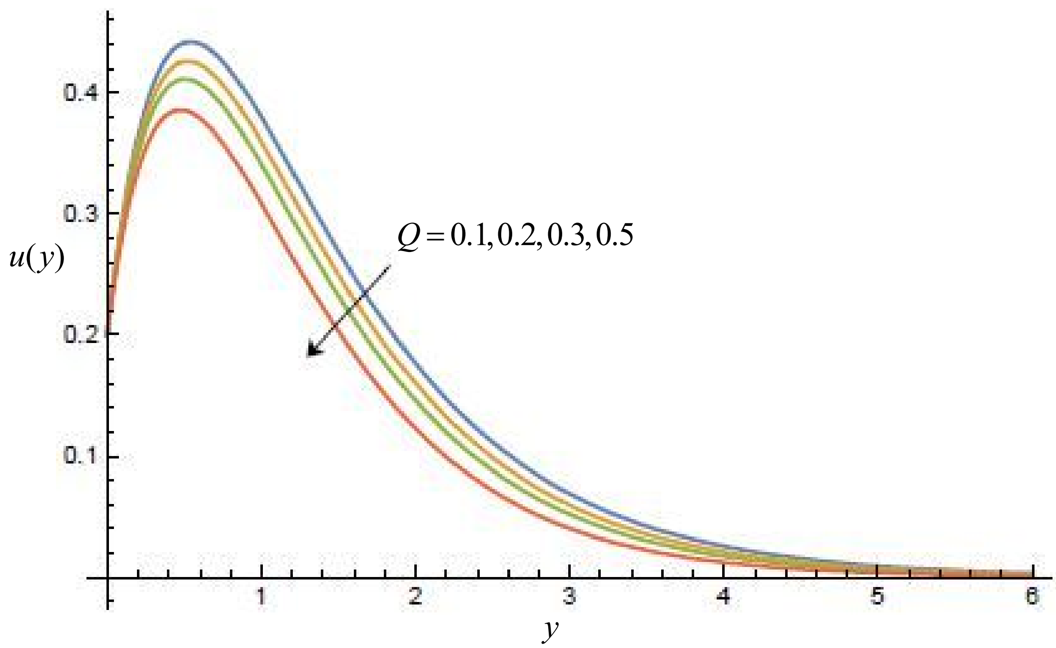


Fig. 11. Influence of $Q$ on velocity profile while other parameters values are $M = 2, Da = 0.5, Pr = 0.71, Gr = 10, Q = 0.2, \omega = 3, up = 0.3, t = 1, \lambda = 0.3$

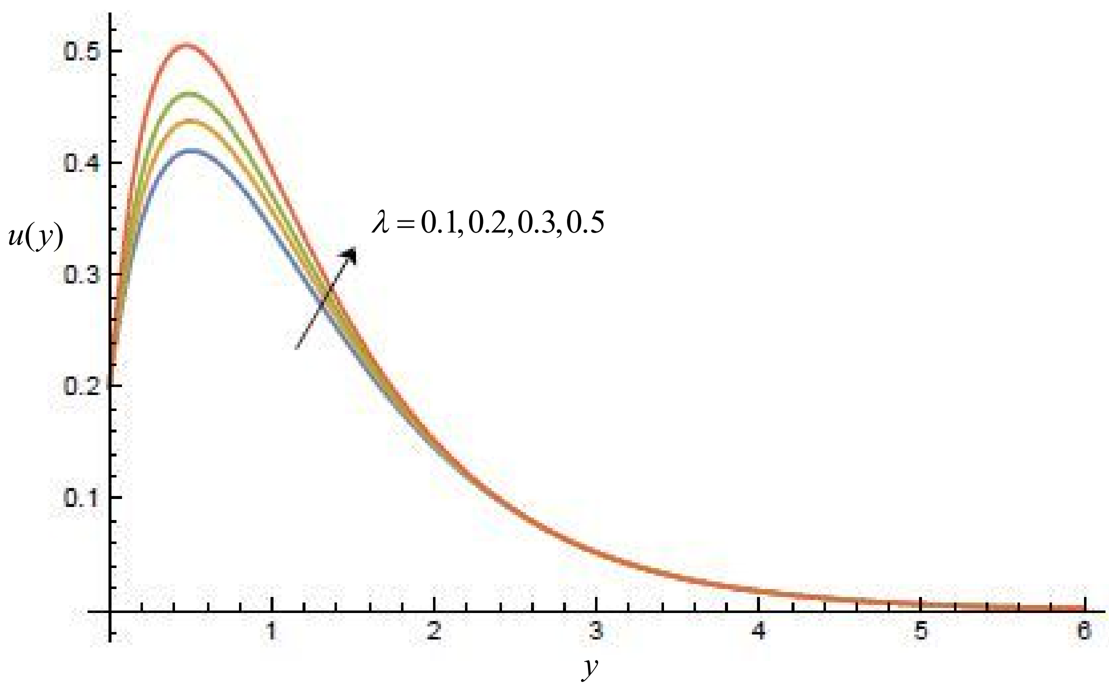


Fig. 12. Influence of $\lambda$ on velocity profile while other parameters values are $M = 2, Da = 0.5, Pr = 0.71, Gr = 10, Q = 0.2, \omega = 3, up = 0.3, t = 1, \lambda = 0.3$

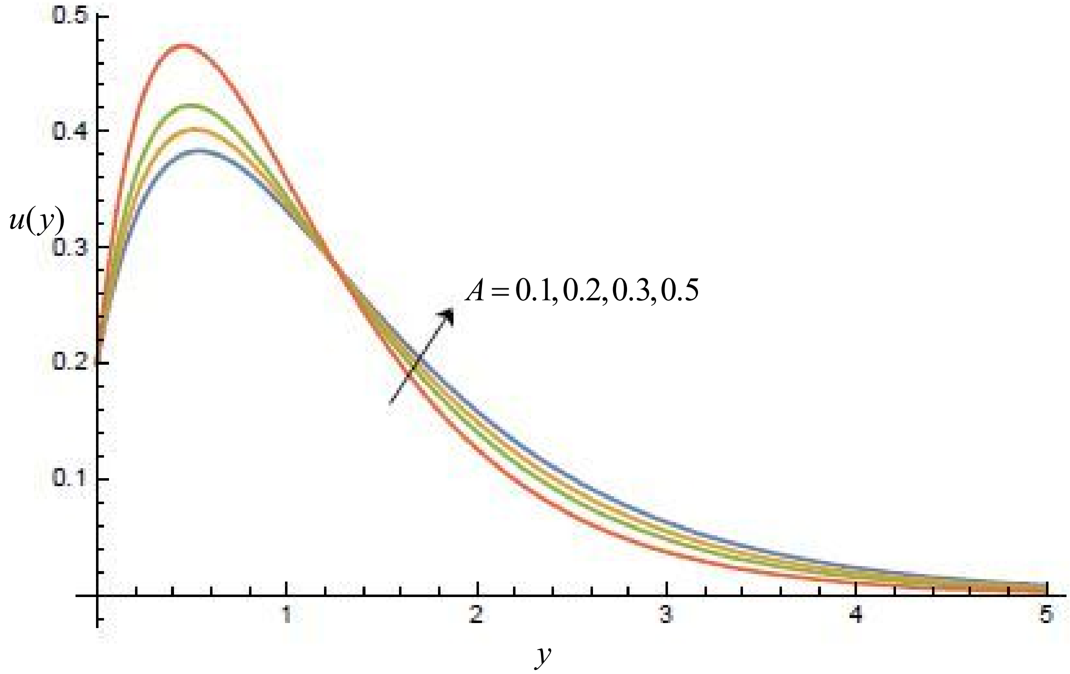


Fig. 13. Influence of $A$ on velocity profile while other parameters values are $M = 2, Da = 0.5, Pr = 0.71, Gr = 10, Q = 0.2, \omega = 3, up = 0.3, t = 1, \lambda = 0.3$

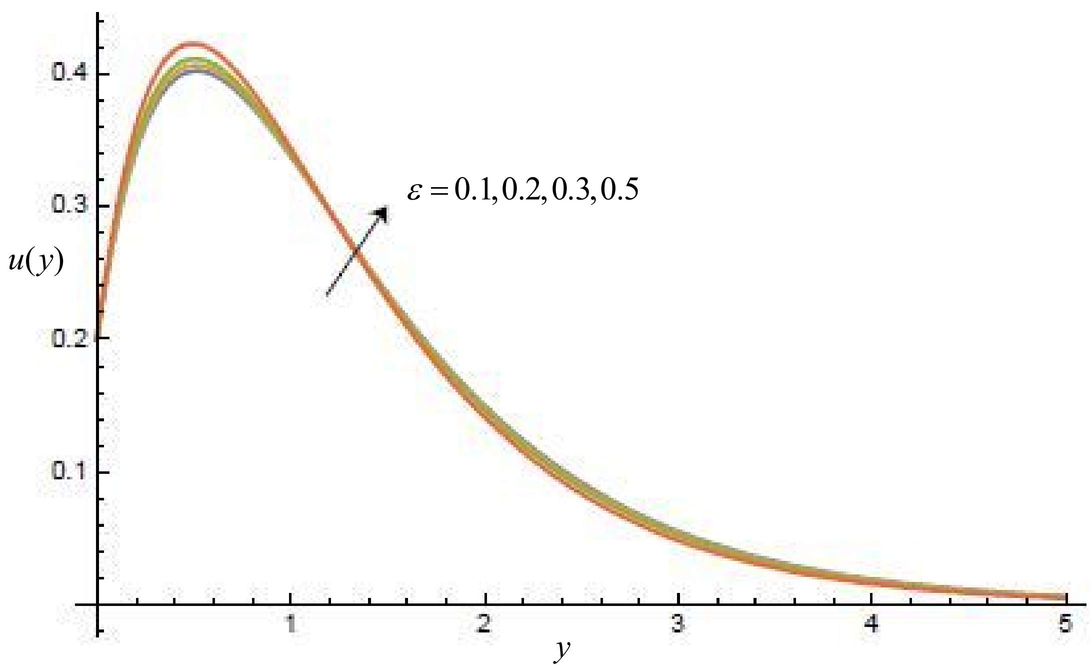


Fig. 14. Influence of $\lambda$ on velocity profile while other parameters values are $M = 2, Da = 0.5, Pr = 0.71, Gr = 10, Q = 0.2, \omega = 3, up = 0.3, t = 1, \lambda = 0.3$

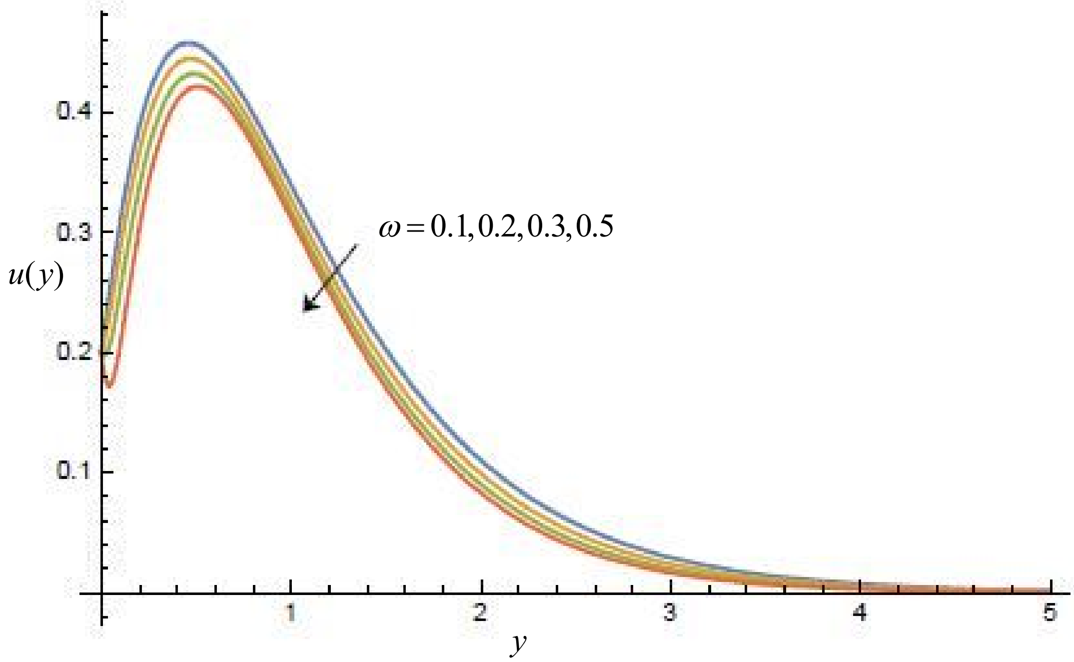


Fig. 15. Influence of $\omega$ on velocity profile while other parameters values are $M = 2, Da = 0.5, Pr = 0.71, Gr = 10, Q = 0.2, \omega = 3, up = 0.3, t = 1, \lambda = 0.3$

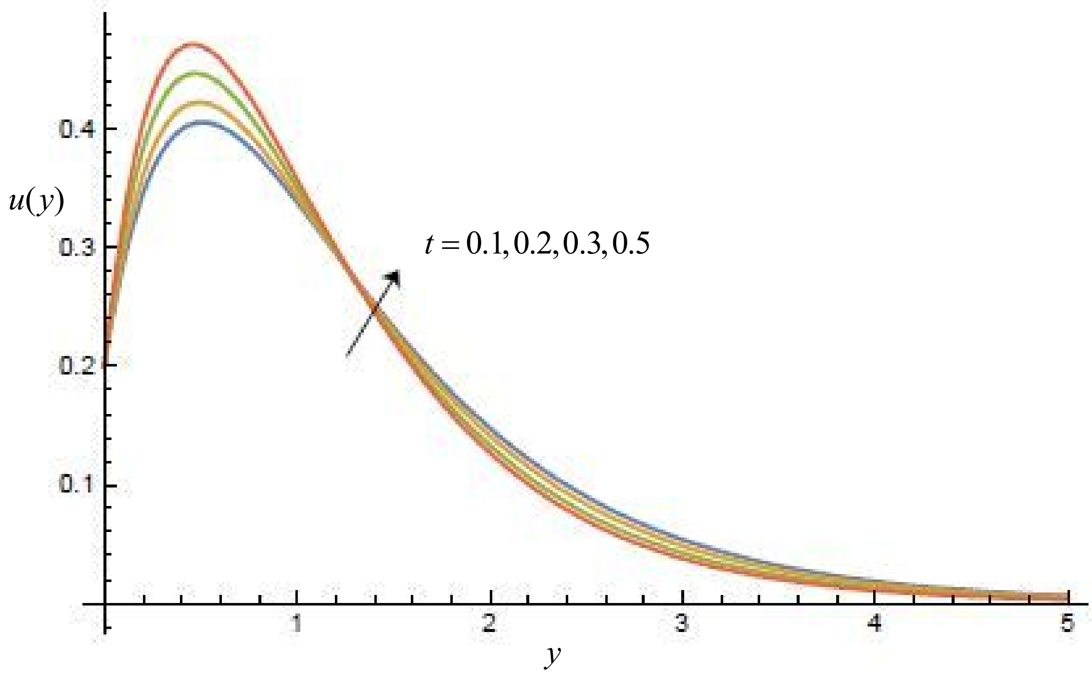


Fig. 16. Influence of $t$ on velocity profile while other parameters values are $M = 2, Da = 0.5, Pr = 0.71, Gr = 10, Q = 0.2, \omega = 3, up = 0.3, t = 1, \lambda = 0.3$

## DISCUSSION

We have solved the formulated problems analytically in equations (17) and (18) and simulations were done and results presented in Figures 1 – 15 graphically. In this section we shall discuss as follows:

Figure 1 depicts the influence of radiation parameter $Q$ on the temperature profile $\theta(y)$ with other parameters $M = 2, Da = 0.5, Pr = 0.71,$ $Gr = 10, Q = 0.2, \omega = 3, up = 0.3, t = 1, \lambda = 0.3$. It can be seen that the temperature profile is maximum at the walls of the plate and for the all values of the radiation parameter $Q$, and it satisfied the set boundary conditions. But we observed that the temperature decrease as boundary layer thickness increases, up to the point that the temperature profile $\theta(y)$ tends to zero as $y \to \infty$.

In Figure 2 it can be observed that there is an influence of suction parameter $A$ on the temperature profile $\theta$ with other parameters $Gr = 10, Q = 0.2, \omega = 3, up = 0.3, t = 1, \lambda = 0.3$ $M = 2, Da = 0.5, Pr = 0.71,$. It showed that as the suction parameter value increase the temperature profile decreases due to the fact that suction effect helps to inhibit the heat convection. It is highest at the wall but decrease as the thickness of the wall increase to the point that the suction cannot help to reverse the heat flow.

We can clearly see the influence of the small positive constant $\varepsilon$ on the temperature profile in Figure 3. It is shown that the temperature profile was maximum at $y = 0$ which agrees with the boundary conditions set out irrespective of the $\varepsilon$ value but it began to decrease over time as the boundary layer increase and the flow with highest $\varepsilon$ value tends to converge fast than the rest as $y \to \infty$.

The influence of magnetic field $M$ on velocity profile $u(y)$ is depicted in Figure 6. It is observed that the velocity is $u = 0.2$ at the start of the boundary layer $y = 0$ and grew to the peak before decreasing to a minimum level as the boundary thickness is increases. It is also noticed that the increasing value of the magnetic field parameter tends to reduce the peak thereby decreasing the velocity profile to a new level as $y \to \infty$. What causes the exponential decrease in the velocity profile is due to Lorentz force, an applied force perpendicular to the direction of the flow. Figure 7 It can be seen that the velocity profile $u(y)$ is influenced by the increase values of the initial velocity parameter $up$. The velocity profile increase from the start of the boundary and grew to the peak before decreasing as the boundary layer increase as the flow increase to zero as $y \to \infty$ which physically agrees with set boundary conditions within the research framework.

Figure 8 shows the influence of permeability parameter on the velocity profile $u(y)$. The figure show that the fluid velocity increases significantly with an increase in Darcy parameter $Da$. It is due to the fact that when we increase Darcy number, it increases the size of the pores inside the porous medium by which the drag force decreases and thus the velocity increases.

Figure 9 shows that increase in the values of Prandtl parameter $Pr$ decrease the velocity rapidly near the wall of plate due to specific heat capacity which is far more than that of the thermal conductivity. The velocity is seen to decrease greatly in the momentum boundary layer thickness. In Figure 10, the velocity profile is been influenced by the increase in Grashof number $Gr$. It is a fact that as the Grashof number increase the velocity profile also increase and physically this is true because it has the tendency to increase the thermal effect. This give rise to an increase in induced flow and it is noticed that the Grashof number do not have any influence as the fluid move away the boundary surface.

The influence of the increasing values of the heat absorption parameter $Q$ is observed in Figure 11. It is seen that the heat absorption parameter increase lead to a corresponding decrease in velocity profile $u(y)$. This is because of the nature of the fluid and we noticed that the current peak is less than the preceding velocity peak which clearly shows the declining in velocity close to the boundary surface but diminished to zero far from the boundary surface. It is seen that Figure 12 that the velocity profile $u(y)$ increases with increasing values of

Jeffrey fluid parameter $\lambda$. This is of the view that velocity profile increases starting from zero and attain different peak values close to the boundary surface but decreases to zero as the boundary gets larger. And the result agrees with the boundary conditions as stated above.

Figure 13 depicts the influence of the suction parameter $A$ on the velocity profile. It's clearly shown that as the suction parameter constant increase the velocity profile reduces to the circled point thereafter, it start to increase and approaches zero as the boundary layer gets larger, $y \to \infty$.

We noticed in Figure 14 that as the $\varepsilon$ increases the velocity profile also increase to a certain height before start to decelerate as it gets away from the boundary layer. The velocity continuously decreases as the thickness of the boundary increase and over time it diminishes to zero as $y \to \infty$.

Figure 15 shows the influence of oscillation parameter on the velocity profile. It can be seen that as the oscillation parameter $\omega$ increase the velocity profile increased along the boundary up to a maximum level of the velocity before it starts to decrease exponentially as it gets further from the boundary layer. This is so true because from the beginning of the flow with steady oscillation it basic assists the flow to accelerates fast to the peak but diminishes as the boundary layer is increased. Figure 16 depicts the involvement of the time parameter on the velocity profile. It is observed that the velocity slowly attain the maximum value close to the boundary layer before decreasing until it gets to the minimum value at $y \to \infty$.

## CONCLUSION

Analytical solutions are obtained for the MHD Convective Flow of Jeffrey Fluid in Parallel Permeable Moving Plates. One of the plate moving uniformly and the other is with suction at rest. The perturbation method with oscillatory terms attached is used to transform the non-linear partial differential equations to ordinary differential equations which are solved and the results and evaluated analytically and results presented graphically. In the light of the present investigation, we conclude as follows:

(1) The velocity profile $u(y)$ is influenced by the Magnetic field parameter $M$, the velocity profile decrease as the Magnetic parameter increases.
(2) The velocity profile is influenced strongly by the Grashof number $Gr$ increase and it's a case of cooling for $Gr > 0$
(3) Darcy number $Da$ also influence the velocity profile in that it increasing the velocity profile to increase
(4) The Jeffrey parameter $\lambda$ strongly influence the flow velocity close to the wall of the plates
(5) The temperature profile is influenced by the increasing values of the suction parameter, increasing $A$ caused the temperature to decrease.

## REFERENCES

Ahmed, J., Shahzad, A., Khan, M. and Ali, R. 2015. A note on convective heat transfer of an MHD Jeffrey fluid over a stretching sheet. AIP Advances. 5(11):117117.

Ahmad, K., Hanouf, Z. and Ishak, A. 2016. Mixed convection Jeffrey fluid flow over an exponentially stretching sheet with magnetohydrodynamic effect. AIP Advances. 6(3):035024.

Berman, AS. 1953. Laminar flow in channels with porous walls. Journal of Applied physics. 24(9): 1232-1235.

Brinkman, HC. 1949. A calculation of the viscous force exerted by a flowing fluid on a dense swarm of particles. Flow, Turbulence and Combustion,. 1(1):27.

Bunonyo, KW. and Eli, IC. 2019. Oscillatory MHD Viscoelastic Flow in a Porous Channel with Heat in the Presence of Magnetic Field: 100-108.

Bunonyo, KW., Israel-Cookey, C. and Amos, E. 2017. MHD Oscillatory Flow of Jeffrey Fluid in an Indented Artery with Heat Source. Asian Research Journal of Mathematics. 1-13.

Cox, SM. 1991. Two-dimensional flow of a viscous fluid in a channel with porous walls. Journal of Fluid Mechanics. 227:1-33.

Cunningham, RE. and Williams, RJJ. 1980. Diffusion in gases and porous media (vol. 1). Plenum Press, New York, USA.

Emeka, A. 2019. MHD Free Convective Dissipative Flow with Heat Source and Chemical Reaction. International Journal of Applied Science and Mathematical Theory. 5(1):66-75.

Hamza, EA. 1999. Suction and injection effects on a similar flow between parallel plates. Journal of Physics D: Applied Physics. 32(6):656.

Hassanien, IA. and Mansour, MA. 1990. Unsteady magnetohydrodynamic flow through a porous medium between two infinite parallel plates. Astrophysics and Space Science. 163(2):241-246.

Hayat, T., Asad, S., Qasim, M. and Hendi, AA. 2012. Boundary layer flow of a Jeffrey fluid with convective boundary conditions. International Journal for Numerical Methods in Fluids. 69(8):1350-1362.

Hayat, T., Ahmad, N. and Ali, N. 2008. Effects of an endoscope and magnetic field on the peristalsis involving Jeffrey fluid. Communications in Nonlinear Science and Numerical Simulation. 13(8):1581-1591.

Joseph, DD. and Tao, LN. 1966. Lubrication of a porous bearing—Stokes' solution. Journal of Applied Mechanics. 33(4):753-760.

Khalid, A., Khan, I., Khan, A. and Shafie, S. 2015. Unsteady MHD free convection flow of Casson fluid past over an oscillating vertical plate embedded in a porous medium. Engineering Science and Technology. 18(3):309-317.

Kirubhashankar, K. and Ismail, AM. 2014. An Exact Solution of the Problem of Unsteady MHD Flow through Parralel Porous Plates. Int. J. of Adv. in Mech. Automobile Engg. 1(1):39-42.

Nejad, MM., Javaherdeh, K. and Moslemi, M. 2015. MHD mixed convection flow of power law non-Newtonian fluids over an isothermal vertical wavy plate. Journal of Magnetism and Magnetic Materials. 389:66-72.

Singh, CB. and Ram, PC. 1978. Unsteady Magnetohydrodynamic Fluid Flow Through a Channel'. Journal of Scientific Research. 28(2):5-7.

Soundalgekar, VM. and Uplekar, AG. 1986. Hall effects in MHD Couette flow with heat transfer. IEEE Transactions on Plasma Science. 14(5):579-583.

**APPENDIX**

NOMENCLATURE

| | |
|---|---|
| $u', v'$ | Dimensional velocity profile |
| $u_o$ | Perturbed velocity profile |
| $x', y'$ | Dimensional distances |
| $V_o$ | Suction velocity |
| $A$ | Suction constant |
| $Q$ | Heat absorption parameter |
| $Q_o$ | Heat absorption constant |
| $k_T$ | Thermal conductivity of the fluid |
| $Da$ | Darcy parameter |
| $Gr$ | Thermal Grashof number |
| $up$ | Wall dimensionless velocity |
| $B_o$ | Strength of applied magnetic field |
| $Cp$ | Specific heat capacity at constant pressure |
| $M$ | Magnetic parameter |
| $T'$ | Temperature of the fluid |
| $T'_\infty$ | Temperature of the fluid far from the plate |

Greek Symbols

| | |
|---|---|
| $\upsilon$ | Kinematic viscosity |
| $Pr$ | Prandtl number |
| $\mu$ | Dynamic viscosity |
| $g$ | Acceleration due to gravity |
| $\omega$ | Oscillatory frequency |
| $\beta_T$ | Thermal expansion coefficient |
| $\theta$ | Dimensionless temperature |
| $\theta_o$ | Dimensionless perturbed temperature |
| $\rho$ | Density of the fluid |

Received: June 13, 2019; Accepted: Sept 12, 2019